Towards Integrated Design and Modeling of High Field Accelerator Magnets

S. Caspi and P. Ferracin

***Abstract*— The next generation of superconducting accelerator magnets will most likely use a brittle conductor (such as Nb_3Sn), generate fields around 18 T, handle forces that are 3-4 times higher than in the present LHC dipoles, and store energy that starts to make accelerator magnets look like fusion magnets. To meet the challenge and reduce the complexity, magnet design will have to be more innovative and better integrated. The recent design of several high field superconducting magnets have now benefited from the integration between CAD (e.g. ProE), magnetic analysis tools (e.g. TOSCA) and structural analysis tools (e.g. ANSYS). Not only it is now possible to address complex issues such as stress in magnet ends, but the analysis can be better detailed an extended into new areas previously too difficult to address. Integrated thermal, electrical and structural analysis can be followed from assembly and cool-down through excitation and quench propagation. In this paper we report on the integrated design approach, discuss analysis results and point out areas of future interest.**

***Index Terms*—Superconducting magnet design, integration, modeling, high field, training.**

I. Introduction

Reports on the design of superconducting accelerator magnets for the past 40 years contain many details on the superconducting cable, magnet cross section, iron yoke, collars and the magnet structure[1]-[5]. Field analysis details are also provided for harmonic calculations and iron saturation. Additional 2D details are common for the coil and structure stress during assembly cool down and excitation aiming at minimizing conductor motion and reduce potential magnet training [6]-[10].

By enlarge there is a clear separation between the magnetic design and the structural design. Separate tasks often lead to designs that conflict and do not take into account each other advantages and strong points. Considering magnet design as one integrated task, where a magnet ends are treated as part of its straight section, where the field, stress, heat transfer and voltage rise are all combined into one multi-physics problem and where iterations and optimizations are integrated into the design, is not only possible today but can be extended into areas yet unexplored. Needless to say that major contributions came from advances in computer software and hardware such as new improved Finite Element computer programs and the ever increasing computational speed and communication. The complexity of superconducting magnet design, not different from many other engineering and physics design tasks, has greatly benefited from such advances. In this paper we highlight the integration between different magnet design programs and show how magnet performance can be better understood. In section II we describe the concept of integration using as an example the design of the LARP IR quadrupole for the LHC. In section III we investigate ideas and possibilities that emerge directly from design integration and look at potential benefits especially to the Nb_3Sn High Field Magnet program at LBNL.

Manuscript received September 20, 2005. This work was supported by the Director, Office of Energy Research, Office of High Energy and Nuclear Physics, High Energy Physics Division, U. S. Department of Energy, under Contract No. DE-AC02-05CH11231.

S. Caspi and P. Ferracin are with Lawrence Berkeley National Laboratory, Berkeley, CA 94720 (phone: 001 510 486 7244; fax: 001 510 486 5310; e-mail: s_caspi@lbl.gov).

II. Integrated Magnet Design

In this section we follow the design integration process from a cable to a complete magnet. We view the entire magnet design as one single process that can provide engineering data on any component at any point during assembly, cool-down, magnet excitation and quench.

A. Creating the Coil Model

Modeling the coil is the first building block of the magnet design. Creating 2D magnet cross-section geometry based on cable size, field strength and quality is therefore the first optimization step of the coil. There are many commercial and in house computer programs that can carry out these tasks – Poisson [11], Roxie [12], Opera 2D [13] and Pklbl [14] to name a few. The output of such program gives the field, harmonics and a short-sample prediction for the magnet performance. Revising the cable size, wedges, layers and the strand physical properties is optimized to maximize the field and minimize its harmonics. An output file with the cable numerical XY coordinates is usually available to be loaded into CAD (Fig. 1).

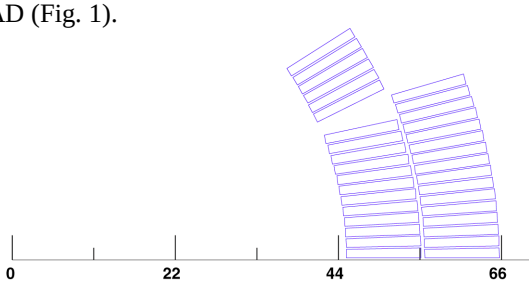

Fig. 1. Typical quadrupole coil cross-section.

With optimized XY coil cross-section coordinates we are ready to proceed and complete the cable windings through both return and lead ends. A computer program such as BEND [15] is an excellent way to do so. Only a few parameters are needed to describe the cable path around the ends, however a user needs to be familiar with the optimization process that minimizes conductor strain. There are many different versions of BEND and users have added their own output files to suit their needs. At LBNL we have placed a Tcl/Tk interface in front of BEND and added several conversion programs that upload the coil geometry into the CAD program ProE [16]. Other conversion programs can create DXF files as well as conductor files suitable for the magnetic program TOSCA [13].

B. Creating the CAD model

The ProE CAD coil model is a set of subassemblies of many parts. In our model each turn is broken into four parts – two straight sections and two end sections (return and lead sides). This is necessary to prevent the CAD system from attempting to smooth out the transition between the end and the straight sections.

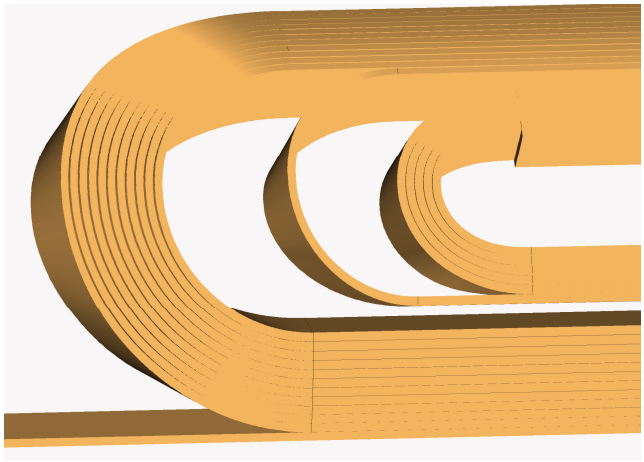

Fig. 2. Typical turns generated by BEND loaded into the CAD ProE program.

Generating the end spacers, shoes, poles and wedges can be done manually by the CAD designer or automatically by a computer program that recognizes turns and assigns their corresponding identical surfaces to the spacer. Applying the same surface to adjacent turns and spacers ensures a perfect match between the turns and the spacers. That program also generates a ProE trail file capable of creating a solid part from its external enclosing surfaces. Typical end spacers in a cos-theta magnet are composed of two cylindrical surfaces (inner and outer radius of each layer) and inside and outside surfaces of the adjacent turns. Whereas inner and outer surfaces of each spacer may be planes as in a racetrack coil or cylindrical as in a cos(ϑ) coil, the other two surfaces adjacent to the turns are described by a set of straight geodesic lines created as rulings by the program BEND. Full advantage is taken of the rulings during manufacturing since they correspond to the position of a straight cutter and can be used in a 5 axis EDM or water-jet machines. Describing each turn within CAD is of great help during the leads design and the layer to layer transition. When such details are not needed the turns can be lumped together into a block that is similar to that of a solid end spacer. The CAD model aside from being the main design tool is also a convenient way to transfer entire magnet assemblies into analysis programs such as TOSCA and ANSYS [17]. That connection aside from being a time saver in model creation reduces human errors and provides an unexpected check of the CAD model quality.

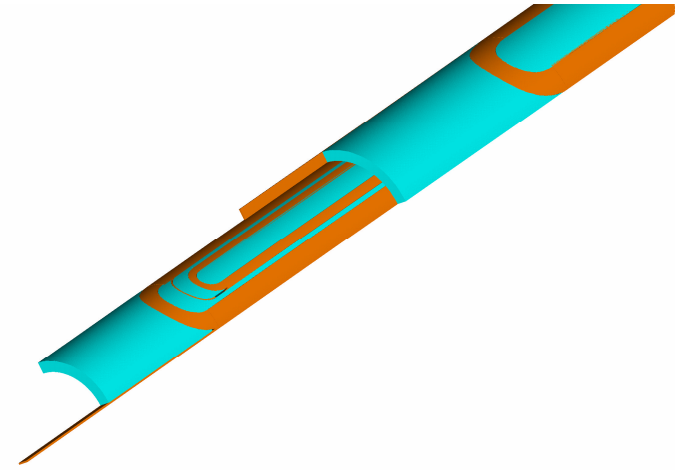

Fig. 3. Typical nesting coils and spacers in CAD ProE.

C. Creating the Magnetic Model (TOSCA)

The CAD ProE magnet assembly can be loaded directly into TOSCA with the help of the MODELLER program. A simple way to do it is through a SAT file. Prior to the transfer we eliminate from the CAD model all non-magnetic components, unimportant details and the coils as well. The coils (8 node bricks) can be added later and read directly into the MODELLER from a modified BEND output file. Setting up the magnetic model is quick and repeating the process can become fairly seamless (Fig. 4).

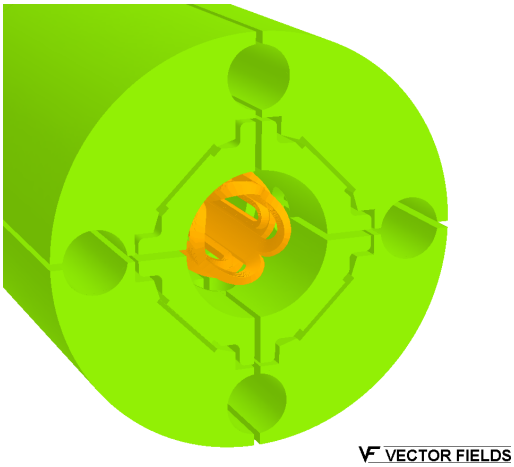

Fig. 4. A 3D TOSCA magnetic model of a quadrupole magnet

Reducing the complexity of the magnetic model setup improves the iron optimization process. Revisions can easily be done in CAD and uploaded into TOSCA. Fig. 5 shows several details in the inner iron pads that went through an optimization process in order to reduce the field in the conductor located over its ends.

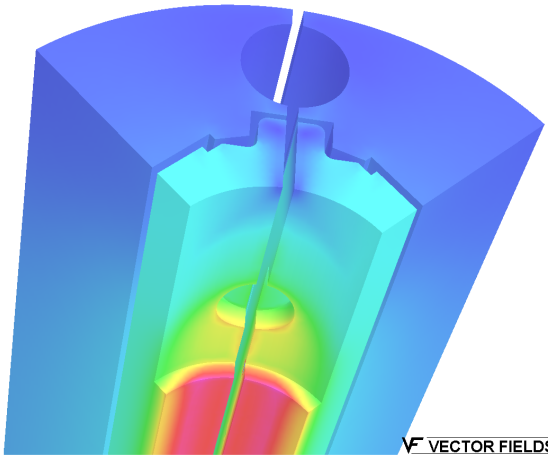

Fig. 5. Magnetic model details of optimized iron features above the coil ends.

D. Creating the Mechanical Model (ANSYS)

The structural ANSYS model was the last step in integrating the design process and was proven to be the most exciting one. An existing ANSYS translator was used to convert ProE solid model assemblies into ANSYS volume assemblies (Fig. 6). So far this conversion was proven to be fast even for large assemblies. Because a magnet contains a large number of parts, the ProE CAD final assembly is broken into a number of sub-assemblies. It is helpful to reduce the complexity of the ANSYS model if the conversion from ProE to ANSYS is done separately for each subassembly. In the final step a specific ANSYS input file is written that reads each subassembly, identifies and sets its components by name, and assigns them material and mesh properties. Meshing is usually generated by a sweep of 20-node structural element (SOLID95) and assembly components are usually allowed to interact via contact elements (TARGE170 and CONTA174) along adjacent surfaces. The successful meshing of a volume and its surfaces, especially between coils and spacers, is a direct consequence of the care taken during their creation in CAD.

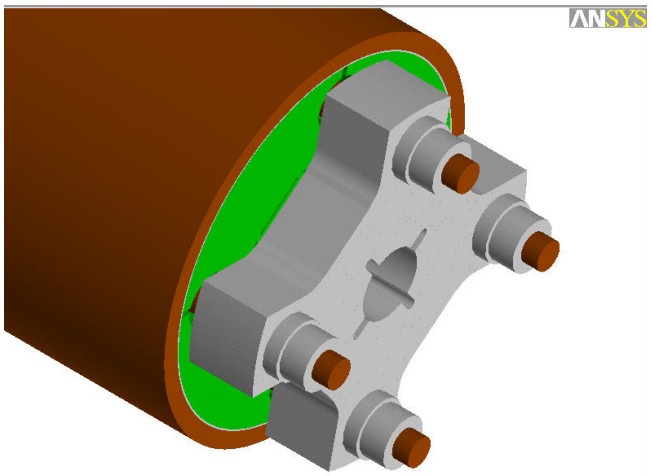

Fig. 6. A 3D ANSYS volumes model, translated from a ProE CAD assembly model, showing the end-plate, yokes and shell (coils not shown).

Fig. 7 shows an important detail where each turn around the magnet end has been extended to meet the spacers inner and outer surfaces. That way proper smoothing between mating components that nest eliminates possible future difficulties during meshing and solving. The analysis solution follows the room temperature assembly, cool-down and the incremental step increase in the Lorentz force. Although generating the Lorentz force can be done within a separate ANSYS magnetic model we have found it to be more convenient to use TOSCA for this process [18]. A simple ANSYS program computes the cancroids of all coil elements. The output file is then read by TOSCA which computes the force per unit volume at each such location (J x B). The three force components are then read back into ANSYS and multiplied by each element volume before being equally divided among all adjacent nodes. We found this process to be convenient, accurate and better suited for coil modification in the ANSYS model and that way extended coil elements in ANSYS with no current density retain a zero Lorentz force.

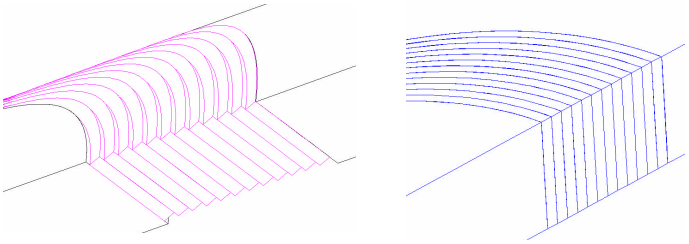

Fig. 7 Stacked coil edges around the ends (left) are extend to meet round smooth surfaces on both coils ID and OD (right)

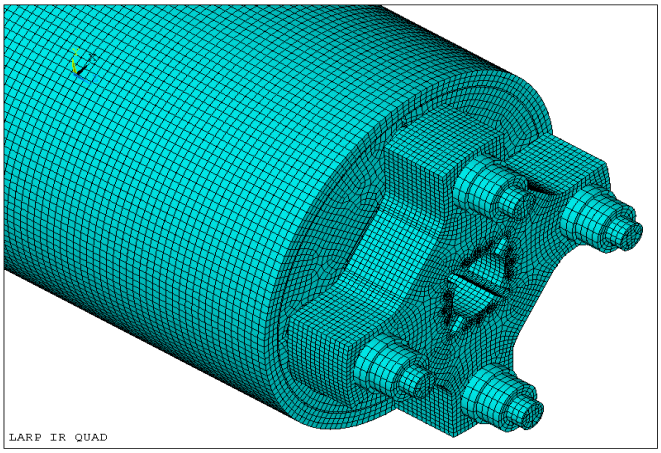

Fig. 8. An ANSYS mesh model of a magnet supporting structural.

With the prescribed design and assembly scheme, improved procedures of magnet design can be devised within a few iterations.

III. MODELING

A. Magnet "ends" and training

One of the most exciting outcomes of integrating the magnet design is the flexibility of providing answers to engineering question previously too difficult to obtain. The inherent integration between the various design elements makes it straight forward and more convenient to give answers to "what if" questions and optimize the design in a way that is better to understand (for example, the impact of flexing end spacers and of cuts in the pole island. We have carried out a 3D analysis on

magnet ends assuming they behave as single solid blocks [19], [20], and, as shown in Fig 9-10, we have also analyzed coils assuming they are composed of individual turns [21]. The analysis was carried out with and without friction between adjacent surfaces including turn to turn. Following the same 2D design approach for maintaining sufficient pre-stress in the pole region to prevent coil separation, it became apparent how difficult it is to apply the same rule to the magnet ends. Avoiding separation between pole turns and end spacers is a complicated task that requires careful application of pre-stress.

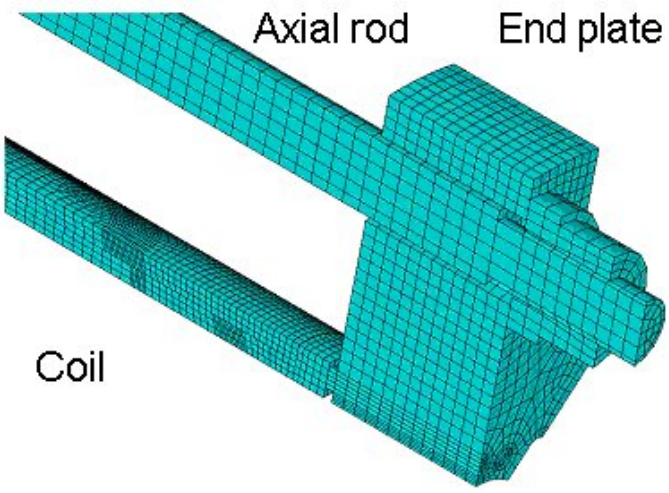

Fig. 9. A detail ANSYS view of the end support structural.

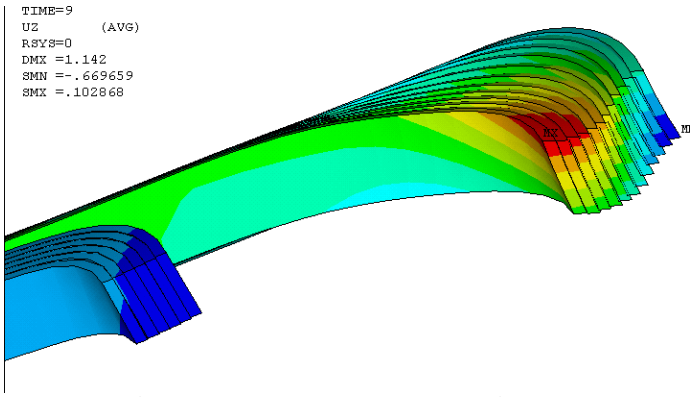

Fig. 10. A deformed coil end region under Lorentz forces modeled with friction between turns.

Fig. 11 demonstrates an exaggerated situation in the end of a quadrupole magnet after cool-down (left) and under a high Lorentz force (right). In both cases the model includes friction and a low compressive axial support. After assembly and cool-down small gaps appear between turns and between turn one and the pole island (Fig. 11 left). We recognize the fact that gap size depend on pre-stress and that in actuality potential gaps in impregnated coils may not occur but replaced instead by turn to turn tension.

At large Lorentz forces (Fig. 11, right) individual gaps collapse into a single larger gap (0.35 mm) located between the pole turn and the island. The large gap size is the result of low axial pre-stress and azimuthal coil separation from the pole island. Fig. 12 shows the progression of that end gap size under different conditions. At 13 kA the gap size increases to 70 μm as a result of "soft" end support. Beyond 13 kA the decrease in azimuthal pole support reduces the axial friction force between turn one and the island (which is under axial tension) causing the island to slide backwards towards the magnet center. As a result the rate by which the end gap changes increases rapidly. We view this instantaneous sliding between the island and the first turn as main source of potential training.

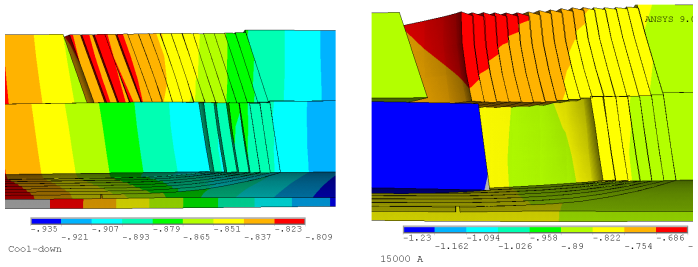

Fig. 11. With an insufficient axial load (left) gaps between turns appear after cool-down. At 15 kA most gaps close but a single larger gap develops between turn one and the pole island (layer 1) causing an instantaneous sliding in the island (right).

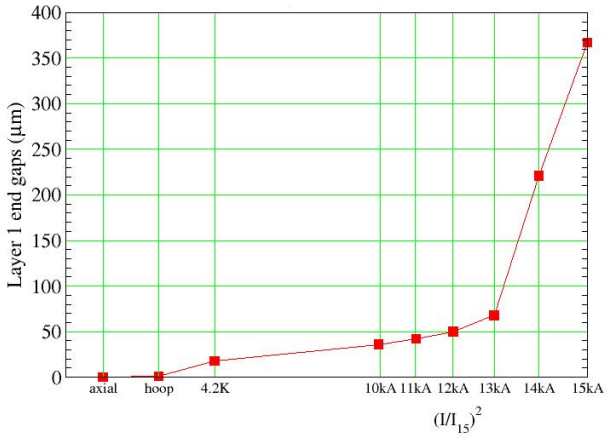

Fig. 12. Axial gap size between pole island and end turn 1 during assembly cool-down and excitation (μ=0.2) with limited axial support. The gap rate change is caused by the island sliding.

The gap size during operation can be completely eliminated with proper axial end support (Fig. 13). The instantaneous sliding between the island and the first turn however cannot be eliminated but delayed to occur beyond the expected short sample level. As shown in Fig. 13, the gap opens up at 14 kA, at least 500 A beyond the short sample value for this magnet.

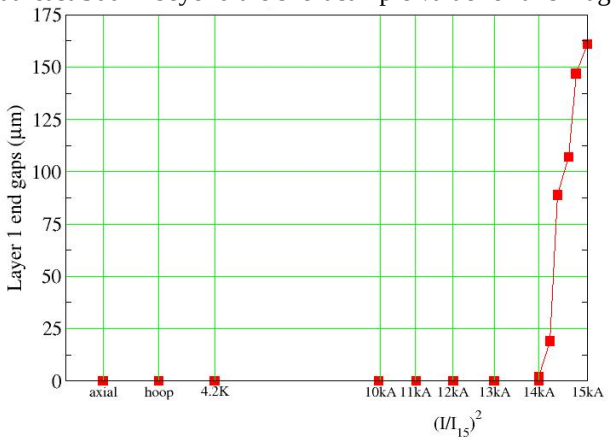

Fig. 13. Axial gap size in the end between pole and turn 1 during assembly cool-down and excitation (μ=0.2) with full end support.

In Fig. 14 we show a side by side view of ends using the same scale for a limited end support (top) and a fully supported end (bottom). As shown, the fully supported end is slightly shorter and has a smaller gap size.

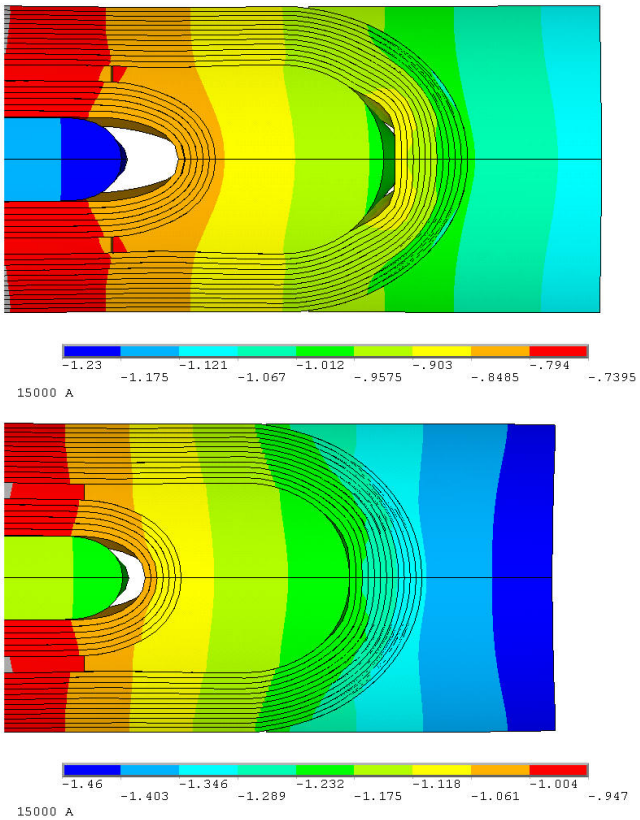

Fig. 14. Axial displacements of inner layer's end-region beyond short sample (0.2 friction factor assumed). Limited axial support (top) and full axial support (bottom).

The magnet integrated design gave us the opportunity to look into this possible training scenario. We are quite aware that until experimentally proven a model remains just that, however, perhaps for the first time, we can quantify R&D details of a possible "stick slip" condition that gives rise to training.

We acknowledge the work of P. Fessia [22] on 3D mechanical modeling of magnet ends.

IV. Quench Propagation

A. *Thermal, Electrical and Mechanical Response*

Another area where integration helps model magnet performance is the simulation of spot-heater experiments within ANSYS. That work yields quench propagation velocities along and across turns, voltage and temperature rise as a function of time and coil tress as a response to a fast rise in temperature. Details covering this work have been reported in the past [23]-[27]. Here too, the combination of CAD coils and surrounding insulation details integrates well into ANSYS and helps provide details on magnet protection issues. Quench propagation calculation is initiated by a momentary rise in the spot heater temperature over its short sample limit. In Fig. 15 (top) a normal zone is shown shortly after a quench started. Half a second later the maximum local temperature reaches 300 K causing a local compressive axial stress of -136 MPa (Fig. 15 bottom). In Fig. 16, the resistive voltage rise across the magnet clearly marks turn to transitions, and in Fig. 18, the computed hot spot temperature response is in good agreement with measurements.

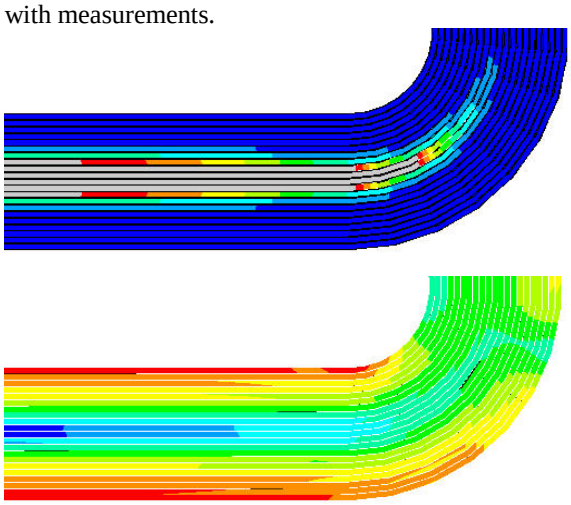

Fig. 15. A coil normal zone after 80 ms with T_{max} = 44 K (top) and a local compressive stress of – 136 MPa after 480 msec when the local temperature reaches 300 K (bottom).

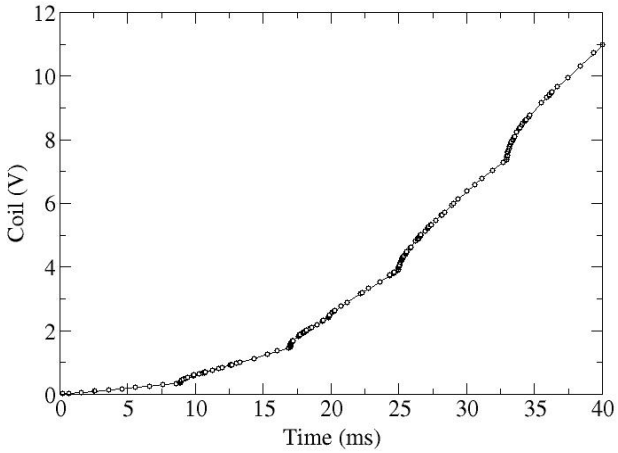

Fig. 16. A typical calculated voltage rise during a quench with distinct turn to turn transitions.

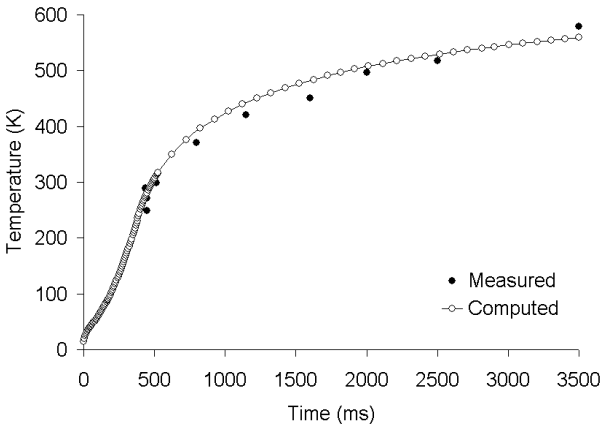

Fig. 18. Measured (black markers) and computed (white markers) hot spot temperature.

V. Future plans

It took many years to reach the point where a magnet design can be fully integrated with its analysis. The evolving process requires at least three professional experts some or all familiar with CAD, TOSCA, ANSYS as well as the overall complexity of superconducting magnet design. We plan to improve and simplify the process by trial and error and especially try and understand the cause of quench initiation that leads to training and ways to prevent it. One such example is to combine ANSYS stick-slip results with quench initiation. We plan to calculate the potential power dissipation in each coil element caused by friction forces and relative motion. The power dissipation may or may not cause a sufficient temperature rise to initiate a quench. However areas where large temperature variations are more likely to occur can be identified and dealt with. We also plan to show that modeling can predict "training", that a path dependent process can be modeled to gradually reduce a magnet stored mechanical energy and improve its performance.

VI. Conclusion

Integration and modeling of present high field superconducting magnets promise designs with substantially more complex features and details. It also promises future magnets to perform with reduced risk and lower costs. Using CAD to capture the design intent and its flexibility in communicating with major finite element program (such as magnetic, structural, thermal and electrical) holds the key in simulating multi-physics problems.

Sliding during magnet excitation results from a simultaneous increase in the axial end Lorentz force, and a decrease in the transverse compressive force on the pole-island. It is caused by the island restoring its free body position and not as a result of coil motion. Sliding cannot be eliminated altogether but can be pushed beyond the short-sample limit by using sufficient axial support.

References

[1] H. Brechna, *Superconducting magnet systems*. Berlin: Springer-Verlag, 1973.

[2] M. N. Wilson, *Superconducting magnets.* Oxford: Clarendon Press, 1983.

[3] Y. Iwasa, *Case studies in superconducting magnets*. New York: Plenum Press, 1994

[4] K. –H. Mess, P. Schmuser, and S. Wolff, *Superconducting accelerator magnet.* Singapore: World Scientific, 1996.

[5] F. M. Asner, *High field superconducting magnets.* Oxford: Clarendon Press, 1999.

[6] H.T. Edwards, "The Tevatron energy doubler: a superconducting accelerator", *Ann. Rev. Nucl. Part. Sci*. 35, pp. 605-660, 1985.

[7] S. Wolff, "Superconducting magnets for HERA", *Proc. 13th Int. Conf. on High Energy Particle Accelerators*, Novosibirsk, Vol. 2, pp. 29, August 1986.

[8] A. Greene, *et al.*, "The magnet system of the Relativistic Heavy Ion Collider (RHIC)", *IEEE Trans. Magnetics*., Vol. 32, no. 4, pp. 2041-2046, July 1996.

[9] A. Devred, *et al.*, "About the mechanics of SSC dipole magnet prototypes", *AIP Conf. Proc*. 249, Vol. 2, pp. 1309-1374, 1992.

[10] O. Bruning, *et al.*, "LHC Design Report v.1: the LHC Main Ring", CERN-2004-003-V1, 2004.

[11] K. Halbach, "A Program for Inversion of System Analysis and Its Application to the Design of Magnets," Lawrence Livermore National Laboratory report UCRL-17436, 1967.

[12] S. Russenschuck, *et al.*, "Integrated design of superconducting accelerator magnets. A case study of the main quadrupole", *Eur. Phys.J. AP* 1, pp. 93-102, 1998.

[13] Vector Fields Limited, 24 Bankside, Kidlington, Oxford OX5 1JE, England.

[14] S. Caspi and R. Schmidt , "Pklbl programs user's manual version 2.0", LBNL report SC-MAG-471, August 1994.

[15] J. Cook , "Strain energy minimization in SSC magnet winding", *IEEE Trans. Magnetics*., Vol. 27, no. 4, pp. 1976-1980, March 1991.

[16] PTC, 140 Kendrick Street, Needham, MA 02494, USA.

[17] ANSYS, Inc., Southpointe, 275 Technology Drive, Canonsburg, PA 15317, USA.

[18] S. Prestemon, Lawrence Berkeley National Lab., Berkeley, CA, private communication, February 2003.

[19] S. Caspi, *et al.*, "Mechanical design of a second generation LHC IR quadrupole", *IEEE Trans. Appl. Supercond*., Vol. 14, no. 2, pp. 235-238, June 2004.

[20] P. Ferracin, *et al.*, "Mechanical analysis of the Nb_3Sn dipole magnet HD1", *IEEE Trans. Appl. Superconduct.*, Vol. 15, no. 2, pp. 1119-1122, June 2005.

[21] S. Caspi, *et al.*, "Design and construction of TSQ01, a 90 mm Nb_3Sn quadrupole model for LHC luminosity upgrade based on a key and bladder structure", presented at *19th International Conference on Magnet Technology*, Genoa, Italy, September 18-23, 2005.

[22] P. Fessia and I. Rodriguez Canseco., "3D FEM mechanical modeling of the head of the LHC Main dipole", presented at *19th International Conference on Magnet Technology*, Genoa, Italy, September 18-23, 2005.

[23] S. Caspi, *et al.*, "Calculating quench propagation with ANSYS®", *IEEE Trans. Appl. Superconduct.*, Vol. 13, no. 2, pp. 1714-1717, June 2003.

[24] R. Yamada, *et al.*, "2-D/3-D quench simulation using ANSYS for epoxy impregnated Nb_3Sn high field magnets", *IEEE Trans. Appl. Superconduct.*, Vol. 13, no. 2, pp. 1696-1699, June 2003.

[25] P. Ferracin, *et al.*, "Thermal, electrical and mechanical response to a quench in Nb_3Sn superconducting coils", *IEEE Trans. Appl. Superconduct.*, Vol. 14, no. 2, pp. 361-364, June 2004.

[26] R. Yamada, *et al.*, "3D ANSYS quench simulation of cosine theta Nb/sub 3/Sn high field dipole magnets", *IEEE Trans. Appl. Superconduct.*, Vol. 14, no. 2, pp. 291-294, June 2004.

[27] http://research.kek.jp/people/wake/